Production DC Screening Techniques for RF Performances of Bipolar ICs*

Sang-Gug Lee
Information and Communications University, Taejon, R. O. Korea
sglee@icu.ac.kr

Sang-Oh Lee and Jin-Su Ko
Samsung Electronics, Korea
solee33@samsung.co.kr
jsko1@samsung.co.kr

Abstract

A novel approach for DC screening of the monolithic silicon bipolar RFICs for noise figure (NF) and power gain (S_{21}) is presented. The proposed technique, which is applied to a 1.8 GHz driver amp, demonstrates excellent correlation between the resistance of a proposed test structure and the NF and S_{21} of the RFIC. This study show that setting a limit on the base resistance of bipolar junction transistors (BJTs) is effective in screening the AC performances of any RFICs as well as discrete transistors.

1. Introduction

The present commercial wireless market is extremely competitive. RFIC cost must be minimized in order to serve high volume markets. One major element of RFIC cost is production testing. Although direct RF testing is technically feasible, it is often very expensive for low cost, high volume products.

The use of DC production testing to screen the RF performance of an RFIC is an attractive alternative to direct RF testing. Even with production RF testing, screening the bad die before the packaging is a sure way of reducing cost. DC testing capabilities are well established, and therefore the cost of adding DC screening techniques for RF performance is minimal.

Section 2 discusses the fundamental relations between the small-signal parameters and the NF and power gain of the BJTs. Section 3 introduces a simple test pattern that is used to estimate the base resistance of the BJTs. Section 4 describes the 1.8 GHz driver amp design. Section 5 presents the experimental correlations obtained between the DC resistance of the test pattern and the NF and power gain of the BJTs and driver amps at 1.8 GHz. Section 6 concludes the paper.

2. NF and S_{21} as a function of BJT small-signal parameters

Many high frequency characteristics of the BJTs strongly depend on the value of base resistance. Using Cooke's method [1], the noise factor of a BJT can be given by

$$F = 1 + \frac{r_b}{R_S} + \frac{r_e}{2R_S} + \frac{(R_S + r_b + r_e)^2}{2\alpha_0 r_e R_S}\left[\left(\frac{f}{Kf_T}\right)^2 + \frac{1}{h_{FE}}\right] \qquad (1)$$

Where r_b is the base resistance, R_S the signal source resistance, r_e the inverse of the transconductance g_m, α_0 the common-base current gain, f the frequency, f_T the cutoff frequency, and h_{FE} the DC common-emitter current gain. The constant K is an empirical factor, typically 1.2 for silicon. For $f \ll f_T$, from eqn. (1), the 4th-term becomes small and/or nearly constant for considerable amount of f_T variation. Typically, the r_b/R_S term dominates the noise factor. Therefore, for a given amount of collector current, the noise factor of a BJT is nearly proportional to the base resistance.

Figure 1 shows a small-signal equivalent circuit of the BJT in common-emitter configuration with a voltage source v_s and load resistance R_L. In Fig. 1, r_π is the input resistance, r_o the output resistance, r_{ex} the parasitic emitter resistance, r_c the parasitic collector resistance, r_μ the base-collector resistance, r_{cs} the collector-substrate resistance, C_π the base-emitter capacitance, C_μ the base-collector junction capacitance, and C_{cs} the collector-substrate junction capacitance. For the circuit shown in Fig. 1, the S-parameters of a BJT can be derived, and S_{21} can be given by [2]

assuming that $r_{cs} > R_L = R_S = 50\Omega > (1/g_m + r_{ex})$, $r_\pi > R_S +$

$$S_{21} = \frac{2\left(\frac{g_m R_L}{1 + g_m r_{ex}}\right)\left(sC_\mu \frac{1 + g_m r_{ex}}{g_m} - 1\right)}{\left(\frac{sC_\pi C_\mu R_L}{C_\pi + C_\mu g_m R_L} + 1\right)\left[\frac{s(r_b + R_S)(C_\pi + C_\mu g_m R_L)}{1 + g_m r_{ex}} + 1\right]} \qquad (2)$$

r_b, $r_\mu > g_m R_L R_S$, and $r_o > R_L$. At some intermediate frequencies that includes RF, above the 1st-pole but below the 2nd-pole, eqn. (2) can be simplified as

$$S_{21} \cong \frac{-2}{s\left(C_\mu + \frac{C_\pi}{g_m R_L}\right)(r_b + R_L)} \qquad (3)$$

Equations (1) and (3) tells us that monitoring the base resistance can be a useful way of assessing the RF

* This research was supported by Samsung Electronics Grant No. AL4102X.

performance of BJTs. Though there are other factors that can degrade the high frequency performances of the BJTs, it is fairly safe to say that the high base resistance guarantees poor NF and power gain.

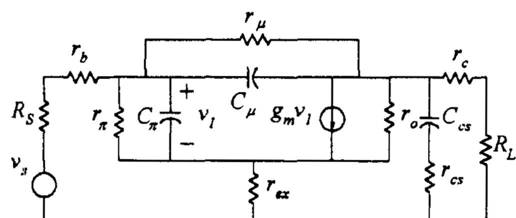

Figure 1. Small-signal equivalent circuit of BJT.

Similarly, many things other than the integrity of the transistors determine the performances of the high frequency integrated circuits. Therefore, good transistors do not guarantee the high frequency performances of the circuits, but a good circuit performance can not be obtained with poor transistors. It is this very idea that the authors of this paper went after and applied to screen the AC performances of RF circuits by the DC measurements of the base resistance.

3. Base-to-base resistance test pattern

The simpler the measurement of the base resistance, the lower the screening cost. For the purpose of screening, it is not the exact value of the base resistance of a specific transistor but the correlation between the base resistance and the ac characteristics of a given circuit. Therefore, a measurement technique that finds out the relative variation of the total base resistance will do the job.

Many aspects of transistor structure determine the total base resistance of a BJT such as the base doping profile, base-width, emitter-length, emitter-width, etc. The base resistance of an advanced NPN bipolar transistor is composed of the pinched and un-pinched P-base resistance, external P^+-base resistance, contact resistance, and poly-silicon base resistance. Typically, the pinched P-base resistance dominates the total base resistance and is subject to process variations in sheet resistivity as well as the lithography of the emitter. Often, the lithography and the sheet resistivity variations can be as large as 50% of their nominal values. While sheet resistivity measurements are simple and routine, the variations in lithography are difficult to monitor. To monitor the base resistance, reflecting the variations of both sheet resistivity and lithography, a test structure has been developed. Figure 2 shows the test structure. The test structure that can be used to estimate the base-to-base resistance of a BJT is an NPN transistor except that the extrinsic P^+-base region is modified to prevent the direct P^+ connection from base to base. Measurement of the resistance between the two bases allows for a relative estimation of the total base resistance, of which the pinched P-base resistance dependent upon the actual lithography and the base sheet resistance.

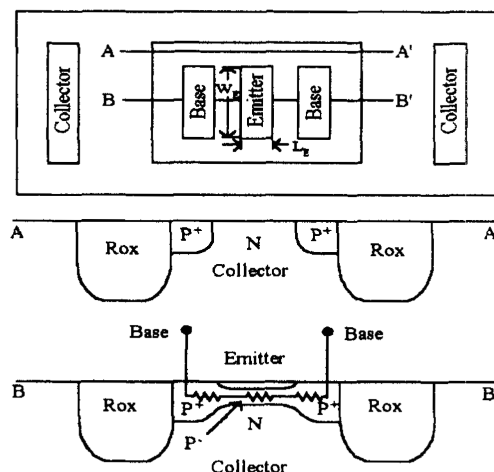

Figure 2. Test structure to estimate the base-to-base resistance of the BJT.

For a double-base normal transistor, the total base resistance can be given by [3]

$$r_b = r_{b,ext} + r_{b,\text{int}} \tag{4}$$

$$r_{b,\text{int}} = \frac{1}{6} \cdot \rho_b \frac{L_E / 2}{W_B W_E} \tag{5}$$

where $r_{b,int}$ is the intrinsic (pinched-P) base resistance, ρ_b the resistivity of the pinched base, L_E the emitter length, W_B the base width, W_E the emitter width. The extrinsic base resistance, $r_{b,ext}$, is composed of the un-pinched P-base, external P^+-base, contact, and the poly-silicon base resistances. Compare to the actual transistor, the total resistance measured across the base-to-base resistance test pattern shown in Fig. 2 can be given by

$$R_{BT} = 2\left(r_{b,ext} + 6 r_{b,\text{int}}\right) \tag{6}$$

where R_{BT} is the test pattern resistance. For the test structure shown in Fig. 2, the resistance of the pinched portion is given by $\rho_b L_E/(W_B W_E) = 2 \cdot 6 \cdot r_{b,int}$.

From eqns. (4) and (6), the test pattern resistance reflects 6 times higher the variations of the intrinsic part of the base resistance over that of the extrinsic parts. The amplification of the pinched base resistance does not seem to be a problem correlating the high frequency characteristics of the BJT. This might be because, the intrinsic part of the base tends to dominate the total base resistance of the typical advanced BJTs and is the most prone to the process variations.

One might say why not use the transistor itself and directly extract the base resistance. Of the BJT model parameters, the base resistance is known as one of the most complicated to extract. Various techniques have been suggested and some of them are based on AC measurements [4, 5]. The more complex the extraction method the longer the measurement time, meaning higher cost for the screening. Furthermore, extracting the base resistance of a transistor involves a test device with

three terminals. The test structure proposed in Fig. 2 requires only two terminals and can be incorporated into an integrated circuits with negligible increase in die area (amount of one additional transistor), for example, by connecting them between two ground pads or the supply pads. The test structure can also be placed in the area of the scribe lines requiring no extra die area.

4. 1.8 GHz driver amp design

Figure 3 shows the circuit schematics of the driver amp. The driver amp is fabricated with a 20 GHz f_T BiCMOS technology. For the limited supply voltage, based on simulatoins, the value of the base voltage V_B is set to 1.9 volts to maximize the P_{1dB} and IP_3.

Figure 4 shows the gain and NF of the driver amp and Table I summarizes the drive amp specifications; objectives, simulations, and measurements.

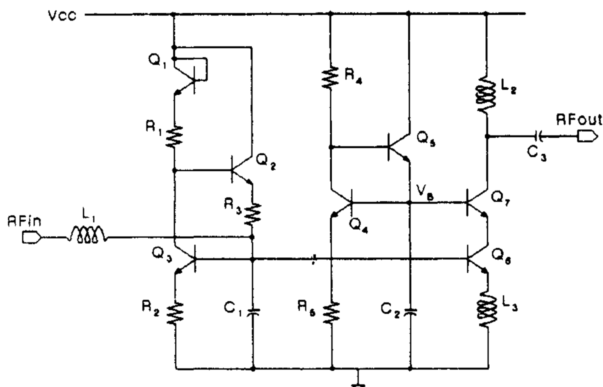

Figure 3. Circuit schematics of the driver amp.

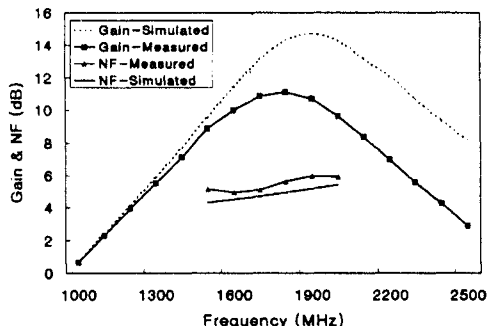

Figure 4. Power gain and NF of the 1.8 GHz driver amp as a function of frequency.

Table 1. Driver amp specifications

Specifications	Objectives	Simulations	Measurements
Frequency	1710–1990 MHz		
S_{21}	12 dB	14.5 dB	13.2 dB
P_{1dB}	7 dBm	9 dBm	6 dBm
NF	5 dB	5.2 dB	5.3 dB
IP_3	25 dBm	25 dBm	23 dBm
I_{CC}	< 37 mA	15.5 mA	16 mA
V_{CC}	3.6 V	3.6 V	3.6 V

5. Correlations results

The correlation between the base resistances and the AC performances of the BJTs and a 1.8 GHz driver amps is investigated. Figure 5 shows the photo of the driver amp, a two-port BJT test pattern, and the base-to-base resistance test pattern on a single chip. In Fig. 5, a 0.5 x 10 μm^2 emitter size is used as the test transistor and the test pattern is the modification of the test transistor

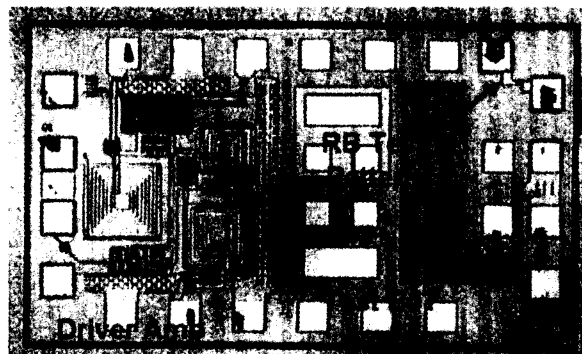

Figure 5. Photo of the 1.8 GHz driver amp, a two-port BJT test pattern, and the base-to-base resistance test pattern on a single chip.

The correlation measurements are done over three wafers for 140 sample dies. The test pattern resistance is measured through the DC measurements. Then, the NF and S_{21} of the transistors and the driver amps are measured for each corresponding test pattern through on-wafer AC measurements. The NF and S_{21} of the test transistors and the driver amps are measured under fixed collector and supply currents, respectively. From eqns. (1) and (3), measuring the AC characteristics under a fixed bias currents removes the g_m variation factor making the NF and power gain more of a function of the base resistance only. Fixed bias currents are also chosen as, more often than not, the integrated circuit designs choose the constant currents as the active device biases. The test transistor is biased at the collector current of 1.25 mA, and the driver amp supply current is adjusted to 16 mA which is the typical value for the 3.6 V supply voltage. The transistors are biased to operate below the high level injection.

Figure 6 shows the NF variation of the test BJT and the 1.8 GHz driver amp as a function of the test pattern resistance. Note that the y-axes are in log scale as the NF is plotted in dB. Therefore, from eqn. (1), the NF is expected to show a logarithmic dependence on the base resistance. As can be seen in Fig. 6, the NF of both BJT and driver amp demonstrates a clear logarithmic dependence on the base resistance, more clearly in the BJT, less in the drive amplifier. The scatter in the driver amp correlation is understandable considering many other components that make up the integrated circuit. Yet, it is surprising that the correlation found at the transistor level can be extended to the integrated circuit.

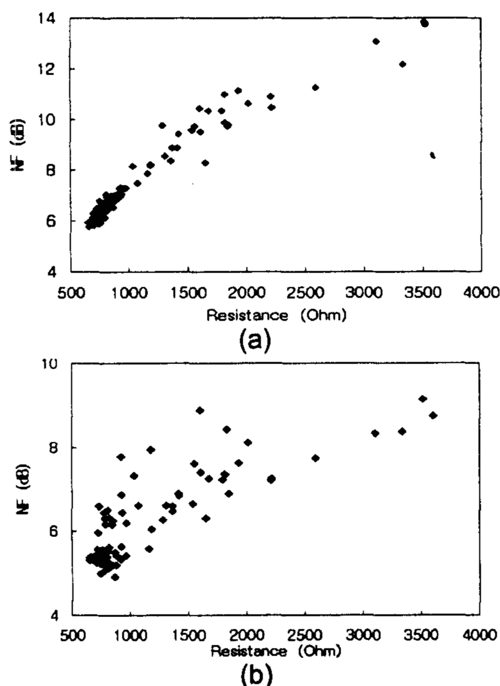

Figure 6. The correlation plot of NF vs. test pattern resistance (a) BJT, I_C = 1.25 mA & V_{CE} = 1 volt; (b) 1.8 GHz driver amp, I_{CC} = 16 mA.

Figure 6-(b) says that the low base resistance does not guarantee the low NF, but low NF can not be obtained with high base resistance. Therefore, the screening based on the base resistance may not be a complete solution for the RF testing, but quite a few of the bad dies can be screened prior to packaging by setting a limit on the base resistance value.

Figure 7 shows the power gain variation of the test BJTs and the driver amps as a function of the test pattern resistance for the same bias conditions as in Fig. 6. Note that the gain shows more scatter compare to the NF even on the transistor level. The scatter is more prominent in the driver amp as expected. Still it can be said, unequivocally, that by setting a limit on the test pattern resistance the power gain of the driver amp can be screened.

The scatter in the BJT power gain correlation, shown in Fig. 7-(a), was expected. From eqn. (3), not only does the power gain a strong function of the base resistance but also a strong function of the parasitic capacitances. The capacitance C_π can be divided as a sum of the diffusion capacitance (C_D) and the emitter-base junction capacitance (C_{je}). With typical S-parameter measurements R_L = 50 Ω. Assuming $C_D >> C_{je}$, and $f_T \cong g_m/(2\pi C_\pi)$, eqn. (3) can be approximated as

$$S_{21} \cong \frac{-2 f_T R_L}{2\pi s(r_b + R_L)} \qquad (7)$$

Eqns. (7) tells us that the power gain of a BJT is a strong function of the cutoff frequency. S_{21} can have considerable variations for the same r_b if f_T varies. As discussed in Section 2, NF tends to have week dependence on f_T at frequencies near 2 GHz.

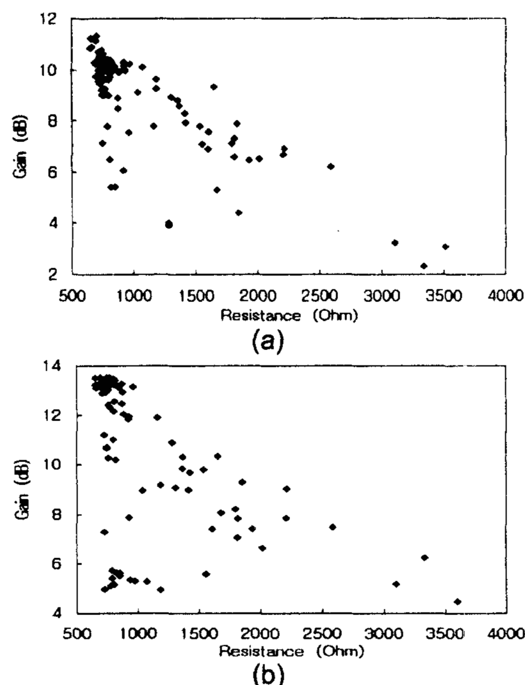

Figure 7. The correlation plot of gain vs. test pattern resistance (a) BJT, I_C = 1.25 mA & V_{CE} = 1 volt; (b) 1.8 GHz driver amp, I_{CC} = 16 mA.

6. Conclusion

Novel techniques for DC screening of RF performance have been presented. The proposed technique uses the variations in the base resistance of the BJT as a sensor to monitor the AC performance fluctuations over the wafer. Study results demonstrate excellent correlation between the noise figure of the BJT and the base-to-base resistance of the proposed test structure. Also, a strong correlation of base resistance to power gain has been found. Furthermore, it has been found that these transistor level correlations can be extended to RFICs. A 1.8 GHz driver amp is used to study the correlation.The proposed techniques are effective in screening any RFIC by setting limits on the AC performance of the active devices used.

7. References

[1] H. F. Cooke, "Transistor Noise Figure," Solid State Design, vol. 4, pp. 137-142, Feb. 1963.

[2] Private communication, John S. Prentice, Harris Semiconductor Co., Melbourne, Florida, USA.

[3] David J. Roulston, Bipolar Semiconductor Devices, New York, McGrawHill 1990, pp. 173-174.

[4] A. Neugroschel, "Measurement of Low-Current Base and Emitter Resistance of Bipolar Transistors," IEEE Trans. Electron Devices, vol. 34, pp. 817-822, Apr. 1987.

[5] S. J. Prasad, "A Method of Measuring Base and Emitter Resistance of AlGaAs/GaAs HBTs," BCTM Tech. Dig., Oct 1992, pp. 204-207